View metadata, citation and similar papers at core.ac.uk

brought to you by CORE

provided by INRIA a CCSD electronic archive server

Detection of Changes in Nonlinear Dynamical Systems using Multiresolution Entropy

Maria E. Torres, Lucas G. Gamero, Carlos E. d'Attellis

To cite this version:

Maria E. Torres, Lucas G. Gamero, Carlos E. d'Attellis. Detection of Changes in Nonlinear Dynamical Systems using Multiresolution Entropy. [Research Report] RR-2812, INRIA. 1996. inria-00073880

HAL Id: inria-00073880

https://hal.inria.fr/inria-00073880

Submitted on 24 May 2006

HAL is a multi-disciplinary open access archive for the deposit and dissemination of scientific research documents, whether they are published or not. The documents may come from teaching and research institutions in France or abroad, or from public or private research centers.

L'archive ouverte pluridisciplinaire **HAL**, est destinée au dépôt et à la diffusion de documents scientifiques de niveau recherche, publiés ou non, émanant des établissements d'enseignement et de recherche français ou étrangers, des laboratoires publics ou privés.

INSTITUT NATIONAL DE RECHERCHE EN INFORMATIQUE ET EN AUTOMATIQUE

Detection of Changes in Nonlinear Dynamical Systems using Multiresolution Entropy

María E. Torres - Lucas G. Gamero
Carlos E. D'Attellis

N° 2812
Février 1996

PROGRAMME 5

Les rapports de recherche de l'INRIA
sont disponibles en format postscript sous
ftp.inria.fr (192.93.2.54)

si vous n'avez pas d'accès ftp
la forme papier peut être commandée par mail :
e-mail : dif.gesdif@inria.fr
(n'oubliez pas de mentionner votre adresse postale).

par courrier :
Centre de Diffusion
INRIA
BP 105 - 78153 Le Chesnay Cedex (FRANCE)

INRIA research reports
are available in postscript format
ftp.inria.fr (192.93.2.54)

if you haven't access by ftp
we recommend ordering them by e-mail :
e-mail : dif.gesdif@inria.fr
(don't forget to mention your postal address).

by mail :
Centre de Diffusion
INRIA
BP 105 - 78153 Le Chesnay Cedex (FRANCE)

Detection of Changes in Nonlinear Dynamical Systems using Multiresolution Entropy

Détection de ruptures dans les systèmes dynamiques non linéaires à l'aide de l'entropie multirésolution

María E. Torres[1] Lucas G. Gamero[2]
Carlos E. D'Attellis[3]

[1]Universidad Nacional de Entre Ríos, Fac. de Ingeniería. CC.57- Suc3 - 3100 Paraná (ER) - Argentine - E-Mail: rnosella@arcride.edu.ar.

[2]Universidad Nacional de Entre Ríos, Fac. de Ingeniería. CONICET. Argentine.

[3]Universidad Nacional de Buenos Aires, Fac. de Ingeniería. Argentine.

The results included in this paper have been presented by the first author in Conferences helded in oportunity of her sojourn at INRIA-Rocquencourt, in the frame of the Cooperation-Project that connects INRIA with Argentine Universities and Scientific Institutes. Coordinators of the project: E. Rofman and R.Gonzalez.

Abstract

This paper deals with a particular aspect of the relation between signal analysis and nonlinear dynamics, which is the detection of changes in parameters of nonlinear dynamical systems from the information obtained using experimental data. We propose a combination of the multiresolution wavelet analysis with the idea of entropy. We show that it provides a new tool, that we calle *multiresolution entropy* (**MRE**), useful for analyzing nonstationary signals and for the detection and localization of slight changes in nonlinear dynamical signals parameters.

Résumé

Cette étude traite d'un aspect particulier des rapports entre l'analyse du signal et les systèmes dynamiques non linéaires: la détection de ruptures dans les paramètres d'une dynamique non linéaire, à partir de l'information fournie par des données expérimentales. Nous proposons une forme de l'analyse en ondelettes qui utilise le concept d'entropie. Nous en déduisons un nouvel outil, que nous appelons *entropie multirésolution* (**MRE**) dont nous montrons l'utilité pour la détection et la localisation de petites ruptures dans les paramètres d'une dynamique non linéaire.

Keywords: Lyapunov exponents, wavelet transform, multiresolution analysis, entropy, nonstationarity, nonlinear systems

Contents

List of Figures

1 Introduction

This paper deals with a particular aspect of the relation between signal analysis and nonlinear dynamics, which is the detection of changes in parameters of nonlinear dynamical systems from the information obtained using experimental data.

When the nonlinear dynamic can be represented by differential equations, there exist a variety of methods that provide a quantitative and qualitative characterization of the system behavior. For example, the spectrum of Lyapunov exponents [10] has proven to be one of the most useful dynamical diagnostic for chaotic system. For systems whose equations are explicitly known there are techniques for computing the Lyapunov spectrum [3], [13]. But when the equations of the nonlinear system are not explicitly given and only experimental data is known, the mentioned methods can not be applied directly [22]. In that case, other approaches to this problem have been proposed. They use the measured data, i.e. time series, and include the computation of the correlation dimension [19], Lyapunov exponents [22], phase space topography [6] and others. It is a common assumption the stationarity of the signal to be analyzed.

This paper deals with changes in nonlinear dynamical systems that produce the experimental data; so the signal analyzed is nonstationary. In [6] a modification of Wolf methods [22] is proposed with the aim of evaluate the Lyapunov exponents taking into account the nonstationarity of the signal. The results obtained indicate that the largest average Lyapunov exponent can be useful in changes detection. The computational cost of this method is very high due to the algorithm itself and the amount of data required (see Section 4). In order to overcome the mentioned drawback, we analyze in this paper the link between Lyapunov exponents and entropy. In fact, as it was pointed out by Pesin [11], under some hypothesis on the nonlinear system both concepts are related each one.

Thus, a) the changes in a nonstationary signal are related to the Lyapunov exponents and b) these exponents are connected with the notion of entropy. But the entropy itself is not useful for analyzing nonstationarities. In fact, as we will show in the examples (Section 4), the computation of the entropy of the signal does not exhibit the changes introduced in the parameters of a nonlinear model.

Looking for an improvement of the entropy performance, we propose in

this paper a new method based on the wavelet transform [8], which is generally acknowledged to be useful for studding nonstationary phenomena and, has shown to be of value in event detection [5]. A combination of the multiresolution wavelet analysis with the idea of entropy is here proposed, and we show that this provides a new tool, called the *multiresolution entropy* (**MRE**), useful for analyzing nonstationary signals and for the detection and localization of slight changes in nonlinear dynamical systems.

The notion of multiresolution entropy has the following advantages: 1) over the entropy, because it is capable to detect changes in a nonstationary signal due to the localization characteristics of the wavelet transform; 2) over the calculation of Lyapunov exponents, because the computational burden is significant lower since the algorithm involves the entropy computation and uses fast wavelet transforms in a multiresolution framework.

The organization of the paper is as follows: in Section 2 a description of the multiresolution analysis and the digital filters used for calculating the wavelet coefficient in fast form are given. The notion of multiresolution entropy is introduced in Section 3. Examples are given in Section 4. In them we show results obtained with the multiresolution approach. First we present nonstationary signals generated simulating nonlinear systems with an imposed time dependent parameter. Then we discuss the results obtained in a real signal, using an electroencephalographic nonstationary signal from epileptic patients, obtained using depth electrodes.

2 Wavelet Transform. Multiresolution Analysis

Suppose that $\psi(t)$ is any basic wavelet, i.e. it verifies [8]

$$\int_{-\infty}^{\infty} \psi(t)dt = 0. \tag{1}$$

The integral wavelet transform of a finite energy signal $f(t) \in L^2(\mathbf{R})$ is defined by [8]

$$(W_\psi f)(b,a) = |a|^{-1/2} \int_{-\infty}^{\infty} f(t)\overline{\psi(\frac{t-b}{a})}dt. \tag{2}$$

We have chosen the polynomial spline wavelet transform introduced by Unser et. al. [18]. The multiresolution representation obtained from this wavelet transform and the digital filters derived allow us the time localization of events in a nonstationary signal in such a way that the requirements enumerated in the Introduction are verified, i.e. good localization and low computational burden. The recursive algorithm for calculating the wavelet coefficients is given by the formulas (6) to (10).

The wavelet function $\psi(t)$ [18] is:

$$\begin{aligned}\psi(t) &= \frac{1}{40320}\,|-\phi(2t+6)+124\phi(2t+5)-1677\phi(2t+4)+\\ &+ 7904\phi(2t+3)-18482\phi(2t+2)+24264\phi(2t+1)-\\ &- 18482\phi(2t)+7904\phi(2t-1)-1677\phi(2t-2)+\\ &+ 124\phi(2t-3)-\phi(2t-4)]\,,\end{aligned}$$

where $\phi(t)$ (the scaling function) is

$$\phi(t) = \begin{cases} 1-|t|+(1/6)|t|^3-(1/3)(1-|t|)^3 & \text{if } |t|\le 1\\ (2-|t|)^3/6 & \text{if } 1\le|t|\le 2\\ 0 & \text{if } |t|>2. \end{cases} \qquad (3)$$

In order to analyze the time-frequency localization properties of the analysis, we will calculate the values of the center and radius of the time and frequency windows and obtain the value of the window area in the time-frequency plane, 2.00268, i.e. almost the optimal value 2 (Cf. [4]). Thus, the selection of this wavelet guarantee a good localization in the time-frequency plane, which was the first of the key points enumerated in the Introduction. The second one, i.e. the numerical implementation of the algorithm, will be considered in the following.

For a given signal $s(t) \in L^2(\mathbf{R})$ initially represented by its polynomial spline coefficients at resolution level 0, the wavelet decomposition is

$$\begin{aligned}s(t) &= \sum_{k=-\infty}^{\infty} c_0(k)\phi(t-k) =\\ &= \sum_{k=-\infty}^{\infty} c_N(k)\phi(2^{-N}t-k)+\sum_{j=1}^{N}\sum_{k=-\infty}^{\infty} d_j(k)\psi(2^{-j}t-k). \qquad (4)\end{aligned}$$

where the numbers $d_1(k), d_2(k), \ldots, d_N(k)$ are the wavelet coefficients, and the sequence $\{c_N(k)\}$ represents the coarser resolution signal at resolution

level N. If this decomposition is carried out over all resolutions levels, the wavelet expansion

$$s(t) = \sum_{j=-\infty}^{\infty} \sum_{k=-\infty}^{\infty} d_j(k) \psi(2^{-j}t - k) \tag{5}$$

is obtained. In each level j the series in (5) has the property of complete oscillation [4], which makes the decomposition useful in applications to time localization of events.

At this point it is convenient to introduce two digital filters that will be used in the algorithm. They are given by the transfer functions

$$B^{-1}(z) = \frac{6}{z + z^{-1} + 4}$$

$$A^{-1}(z) = \frac{5040}{z^3 + z^{-3} + 2416 + 1191(z + z^{-1}) + 120(z^2 + z^{-2})}$$

where z is a complex variable.

As it is usual, we indicate with $b^{-1}(k)$ and $a^{-1}(k)$ the impulse responses of these filters.

Following [18] a fast recursive scheme for obtaining the expansion coefficients in (4) is given by (the symbol * means discrete convolution):

$$c_0(k) = [b^{-1} * s](k) \tag{6}$$

$$c_{j+1}(k) = [v^* * c_j]_{\downarrow 2}(k) \tag{7}$$

$$d_{j+1}(k) = [w^* * c_j]_{\downarrow 2}(k), \tag{8}$$

where

$$v^*(k) = (1/2)[[a^{-1}]_{\uparrow 2} * a * u](k) \tag{9}$$

$$w^*(k) = (1/2)[[a^{-1}]_{\uparrow 2} * u_s * \delta_1](k). \tag{10}$$

and

$$u_s(k) = (-1)^k u(k), \quad \delta_1 * a(k) = a(k-1),$$

$[a]_{\downarrow 2}(k)$ indicates $\ldots, a(-2), a(0), a(2), \ldots$ and $[a]_{\downarrow 2}(k) = a(k/2)$ if k is even and

$[a]_{\downarrow 2}(k) = 0$ if k is odd.

Summing up, the coefficients of the expansion (4) are calculated with the digital filters (9) and (10).

3 Multiresolution Entropy

As it was pointed out, the wavelets have interesting localization properties in the time-frequency plane. The wavelet coefficients corresponding to the level j of the multiresolution analysis are

$$D_j = \{d_j(k), \quad k = 1, \ldots, K_j\}. \tag{11}$$

If the total amount of analyzed data is a power of two, i.e. 2^N, the number of coefficients in the level j is 2^{N-j} due to the decimation effect.

Let us assume for simplicity a fix resolution level and its wavelet coefficients

$$D = \{d(k), \quad k = 1, \ldots, K\}. \tag{12}$$

They are calculated with the method explained in Section 2.

On this set of wavelets coefficients we define a sliding window depending on two parameters: the width $w \in \mathbb{N}$ (an even number), and the sliding factor $\Delta \in \mathbb{N}$. The definition of the sliding window of data is the following:

$$W(m; w, \Delta) = \{d(k), k = 1 + m\Delta, \ldots, w + m\Delta\}, m = 0, 1, 2, ..., M. \tag{13}$$

where Δ and w are selected such that $w \leq K$ and $(K - w)/\Delta \in \mathbb{N}$. For example, if $w = 10$ and $\Delta = 5$, $S(1; 10, 5) = \{d(1), d(2), \ldots, d(10)\}$, $S(2; 10, 5) = \{d(6), d(7), \ldots, d(15)\}$, etc. The center of the window (13) is $d(w/2 + m\Delta)$.

For each window $W(m; w, \Delta)$ we take a partition

$$s_0 = s(m) < s_1 < s_2 < \ldots < s_L = S(m),$$

where

$$s(m) \hat{=} \min\left[W(m; w, \Delta)\right] = \min_k \left[\{d(k), k = 1 + m\Delta, \ldots, w + m\Delta\}\right]$$

$$S(m) \hat{=} \max\left[W(m; w, \Delta)\right] = \max_k \left[\{d(k), k = 1 + m\Delta, \ldots, w + m\Delta\}\right]$$

and consider the set $\{I_l = [s_{l-1}, s_l),\ l = 1, \ldots, L\}$, of disjoint intervals such that

$$W(m; w, \Delta) = \overline{\bigcup_{l=1}^{L} I_l}. \tag{14}$$

We will indicate $p^m(I_l)$ the probability that the wavelet coefficient $d(k) \in W(m; w, \Delta)$ belong to the interval I_l. This probability is the quotient between the number of wavelets coefficients of $W(m; w, \Delta)$ in I_l and the total number of wavelets coefficients in $W(m; w, \Delta)$.

Now we define the *multiresolution entropy* (**MRE**) as

$$H(m) = -\sum_{l=1}^{L} p^m(I_l) \log(p^m(I_l)), \quad m = 0, 1, \ldots, M. \tag{15}$$

In this way we obtain the entropy evolution of the wavelet coefficients at the considered resolution level.

In the general case it will be $M = M_j$, $D = D_j$, $K = K_j$, $L = L_j$, $W(m; w, \Delta) = W_j(m; w, \Delta)$, $p^m = p_j^m$ and $H(m) = H_j(m)$.

As it will be shown in the next section, if we plot at each level the MRE (15) vs. time, considering the points $\{w/2 + m\Delta, H_j(m)\}$, $m = 1, \ldots, M_j$, this approach has the localization properties of the wavelets, so it is useful in detecting changes. Moreover, its computational burden is lower than the methods based on Lyapunov exponents.

4 Results and Discussion

We will analyze four examples: in the first three ones, the signals are generated using known models in which we impose a change in one parameter; the fourth one corresponds to an electroencephalographic signal from an epileptic patient. In the simulated cases, we also discuss the behavior of the MRE and the entropy of signals obtained for constant parameters values, under a linear modification of one of the output states of the system. As we will show, the MRE presents a clear change at the three first resolution levels in most of the simulated models. Even if the entropy shows a similar behavior, it is not so clear in some cases. It will be shown that in almost all the cases, the MRE keeps invariant in face to a linear change of the output signal, that not affect in an obvious way the original signal's graphic.

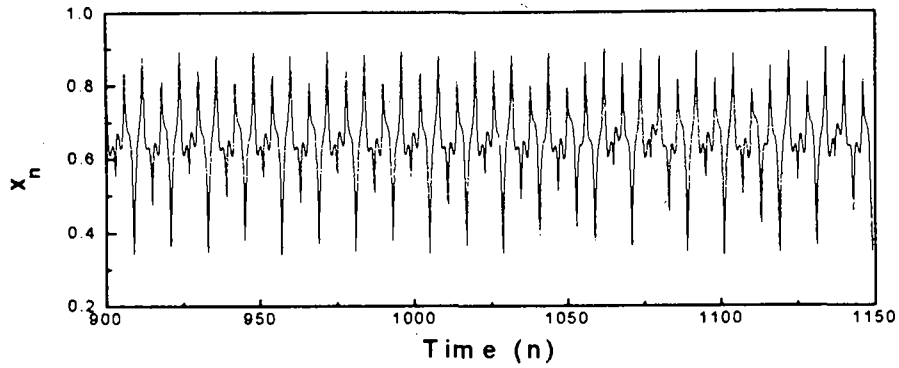

Figure 1: Temporal evolution of the cuadratic map (eq. 16), with linear variation of the parameter a_n as in (eq. 17), with $a_1 = 3.57$, $a_2 = 3.60$, $n_1 = 1024$, $n_2 = 1048$, and initial condition $x_1 = 3.60$.

4.1 Case I: Signals generated by a discrete models

4.1.1 Simulation performed using the cuadratic map model

First we present a simulation performed using the cuadratic map model

$$x_{n+1} = a_n x_n (1 - x_n) \tag{16}$$

i) Consider parameter a_n evolving in order to produce a change at the dynamic behavior as

$$a_n = \begin{cases} a_1 & if \quad n < n_1 \\ a_1 + [(n - n_1)(a_2 - a_1)/(n_2 - n_1)] & if \quad n_1 \leq n \leq n_2 \\ a_2 & if \quad n > n_2 \end{cases} \tag{17}$$

Figure 1 shows the temporal evolution of the cuadratic map with a linear variation of the parameter a_n at a band where a chaotic attractor is present [15], with $a_1 = 3.57$, $a_2 = 3.60$, $n_1 = 1024$ and $n_2 = 1048$. The entropy does not exhibited any change worthy of notice in its evolution (Figure 2). However, the MRE evolution shows an important change at levels 1,2 and 3 (Figure 3).

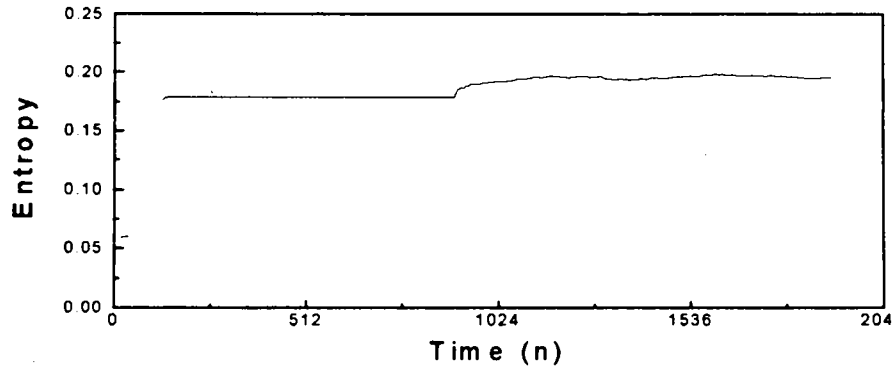

Figure 2: Entropy temporal evolution of the cuadratic map signal (Figure 1). It does not exhibited any change worthy of notice in its evolution

ii) We assume a linear perturbation *at the output* x_n of the system (16) with constant parameter a_n. As a first case, we perform a multiplication by a factor b_n and we consider:

$$y_n = b_n\ x_n;\ where\ b_n = \begin{cases} 1 & if \quad n \leq n_o \\ b & if \quad n > n_o \end{cases} \tag{18}$$

We obtain the behavior shown in figure 4, for $a_n$constant, $a_n = 3.60$, $b = 1.1, n_o = 1024$, and initial condition $x_1 = 3.60$. In figures 5 and 6 can be appreciated that the entropy presents a smooth modification, like a lobe, around n_o, but the MRE does not present any *jump* at n_o at its three first levels.

iii) As a third case, we add a value c_n to the output:

$$y_{n+1} = x_{n+1} + c_n; where\ c_n = \begin{cases} 0 & if \quad n \leq n_o \\ c & if \quad n > n_o \end{cases} \tag{19}$$

In figures 7, 8, 9 we show y_n evolution and its entropy and MRE evolutions respectively, for a_n, n_o and x_1 as before and $c = 0.1$ ($> 10\ of\ Max[x_n]$). Again the entropy presents a lobe around n_o,

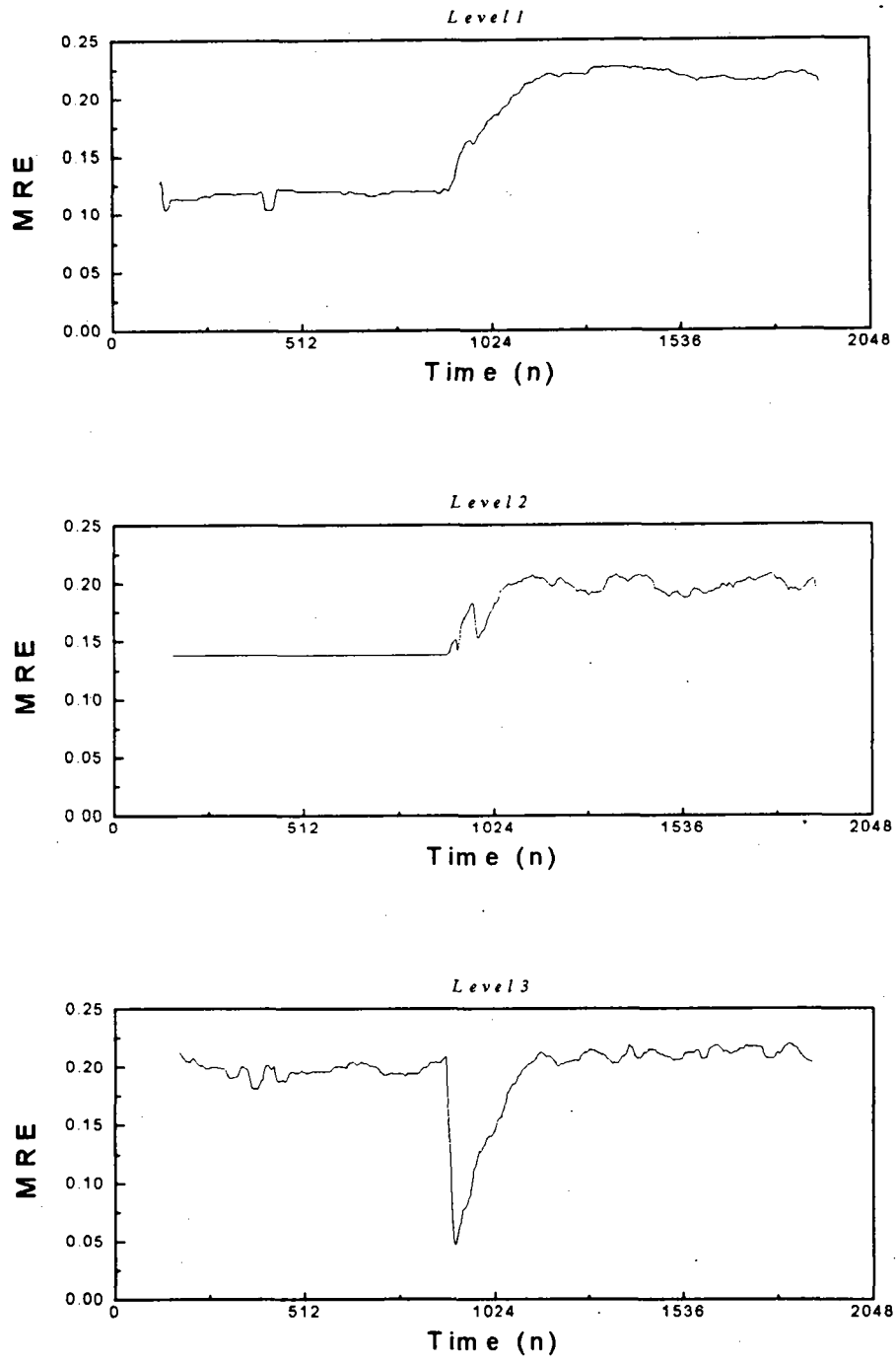

Figure 3: MRE evolution of the cuadratic map signal Figure 1. It shows an important change at levels 1,2 and 3.

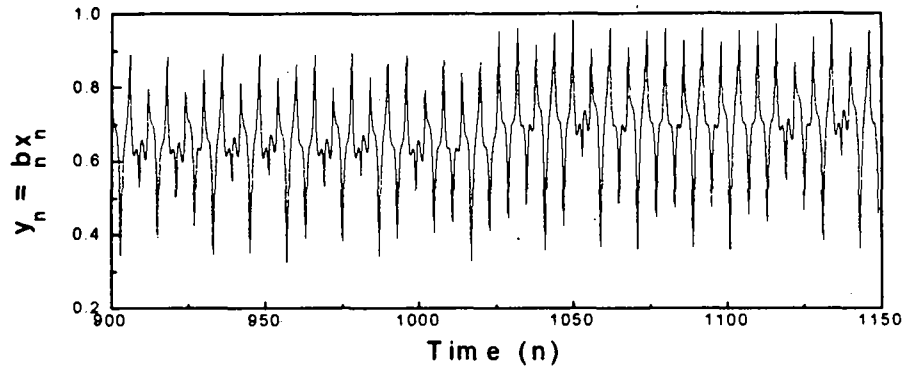

Figure 4: Temporal evolution of the cuadratic map (eq. 16), with linear perturbation of the output x_n as in (eq. 18) , with $a_n = 3.60$, $b = 1.1$, $n_0 = 1024$ and initial condition $x_1 = 3.60$.

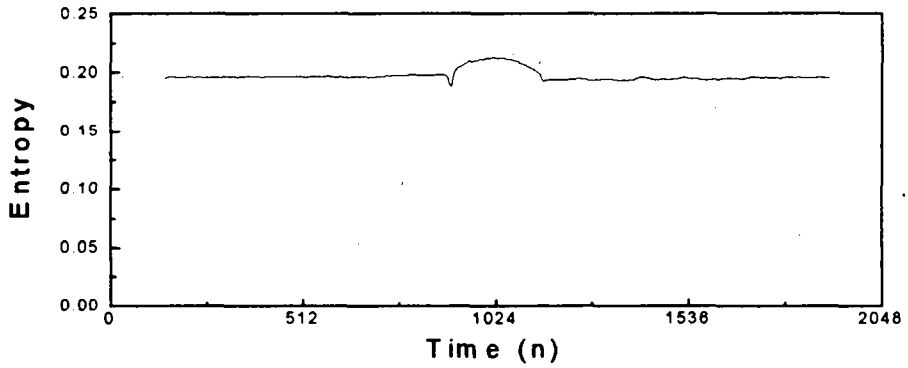

Figure 5: Entropy temporal evolution of the cuadratic map signal(Figure 4). It presents a smooth modification, like a lobe, around n_0.

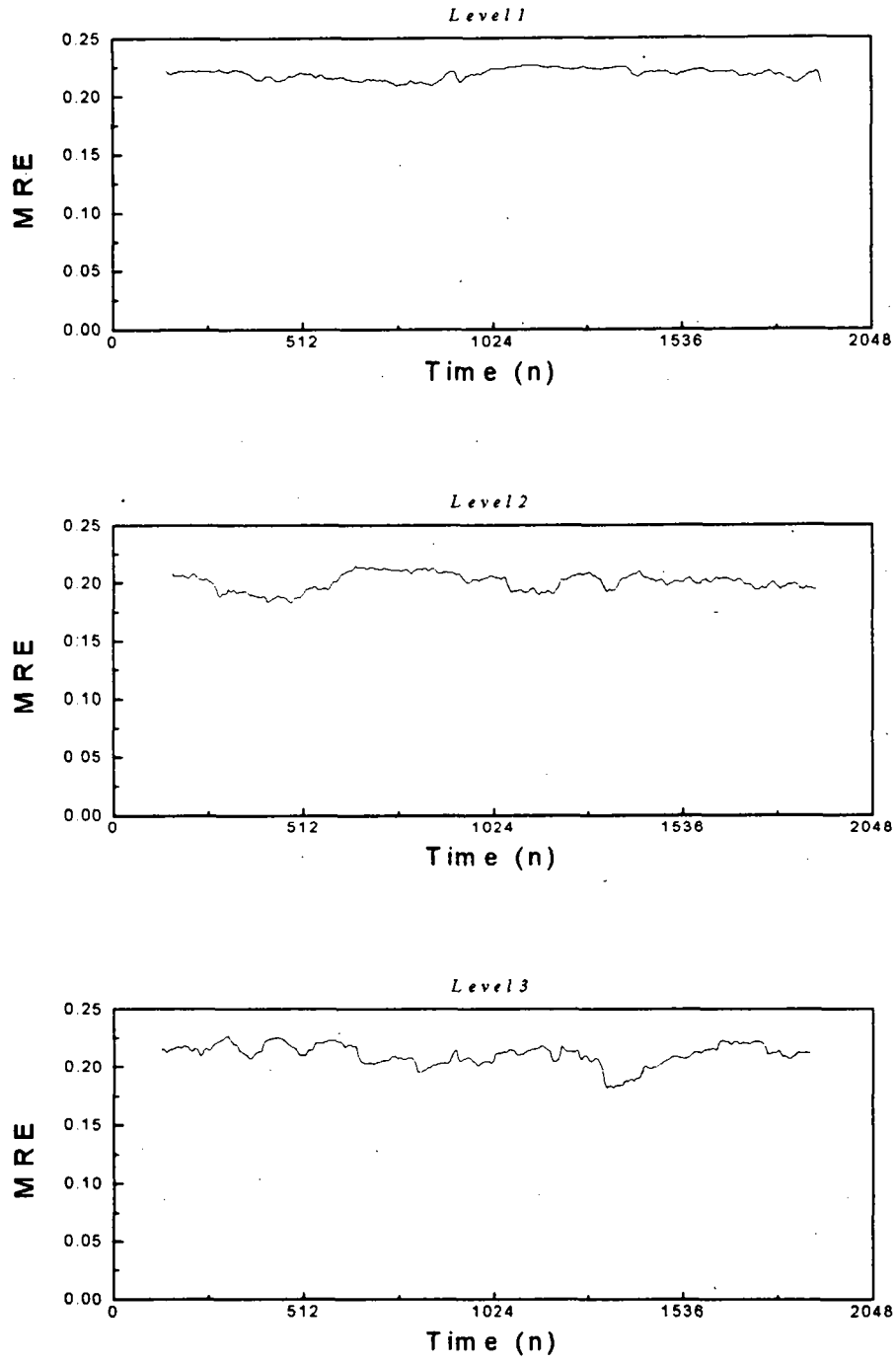

Figure 6: MRE time evolution of the cuadratic map signal in Figure 4. The MRE does not present any *jump* at n_0.

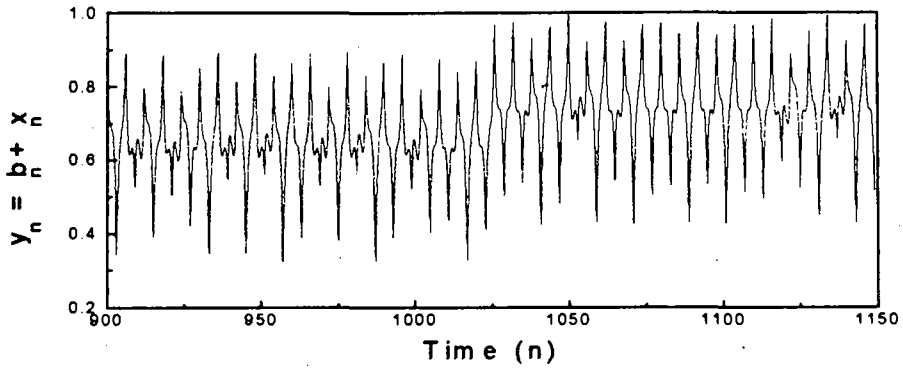

Figure 7: Temporal evolution of the cuadratic map (eq. 16), with linear perturbation of the output x_n as in (eq. 19), for a_n, n_o and x_1 as before and $c = 0.1$.

and the MRE keeps without any perceptible *jump* at its three first levels, even if something appears at the fourth one

4.1.2 Simulation performed using Henon map.

$$\begin{aligned} x_n &= 1 + y_{n-1} - a_n . x_{n-1}^2 \\ y_n &= b \ . \ x_{n-1} \end{aligned} \tag{20}$$

i) In figure 10 we show the signal corresponding to the first state of the system, x_n, with fix parameters $a = 1.4$ and $b = .3$. In figure 11 we show its entropy evolution and in figure 12 the MRE entropy evolution.

ii) Now, we consider the signal corresponding to the first state of the system, x_n, with parameter a_n changing linearly as in eq. 17, with $a_1 = 1.4$, $a_2 = 1.080744879$, $n_1 = 1312$, $n_2 = 1348$, and parameter $b = .3$. In figures 13 and 14 the entropy and MRE time evolution are shown. The drops at the place where the changes of the parameter a_n are imposed are clearly shown at the two first levels of the MRE. At the third level we observe that the MRE increases its value, being coincident the temporal localization with what is observed at the other two resolution levels.

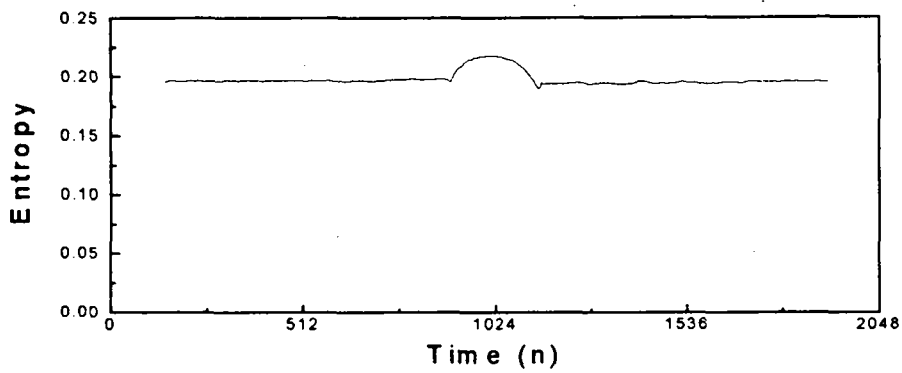

Figure 8: Entropy temporal evolution of the cuadratic map signal at Figure 7. Again the entropy presents a lobe around n_o.

iii) In figures 15. 16, 17 and 18 we show the entropy and MRE time evolutions for the signals obtained imposing to the output x_n of Henon Map (eq.20), with constant parameters $a = 1.4$, $b = .3$, as in equations 18 and 19 , at $n_o = 1000$. There is any clear evidence of the modification imposed to the signal.

In all the cases we have selected small linear variations in the output or in the parameter, so that it could not be detected by simple visual inspection of the signal

4.2 Case Ib: Signal generated by a continuous model

In this example we use the Lorenz equations

$$\begin{aligned} \dot{x}\,(t) &= \sigma\,[y(t) - x(t)] \\ \dot{y}\,(t) &= x(t)\,[R(t) - z(t)] - y(t) \\ \dot{z}\,(t) &= x(t)y(t) - bz(t) \end{aligned} \tag{21}$$

with parameters $\sigma = 16.0$, $b = 4.0$. $R(t)$ is used as the variable parameter changing according to a continuous version of (eq. 17), with $R_1 = 45.92$, $R_2 = 55.92$, $t_1 = 980$ and $t_2 = 1020$. The Lyapunov spectrum for the initial

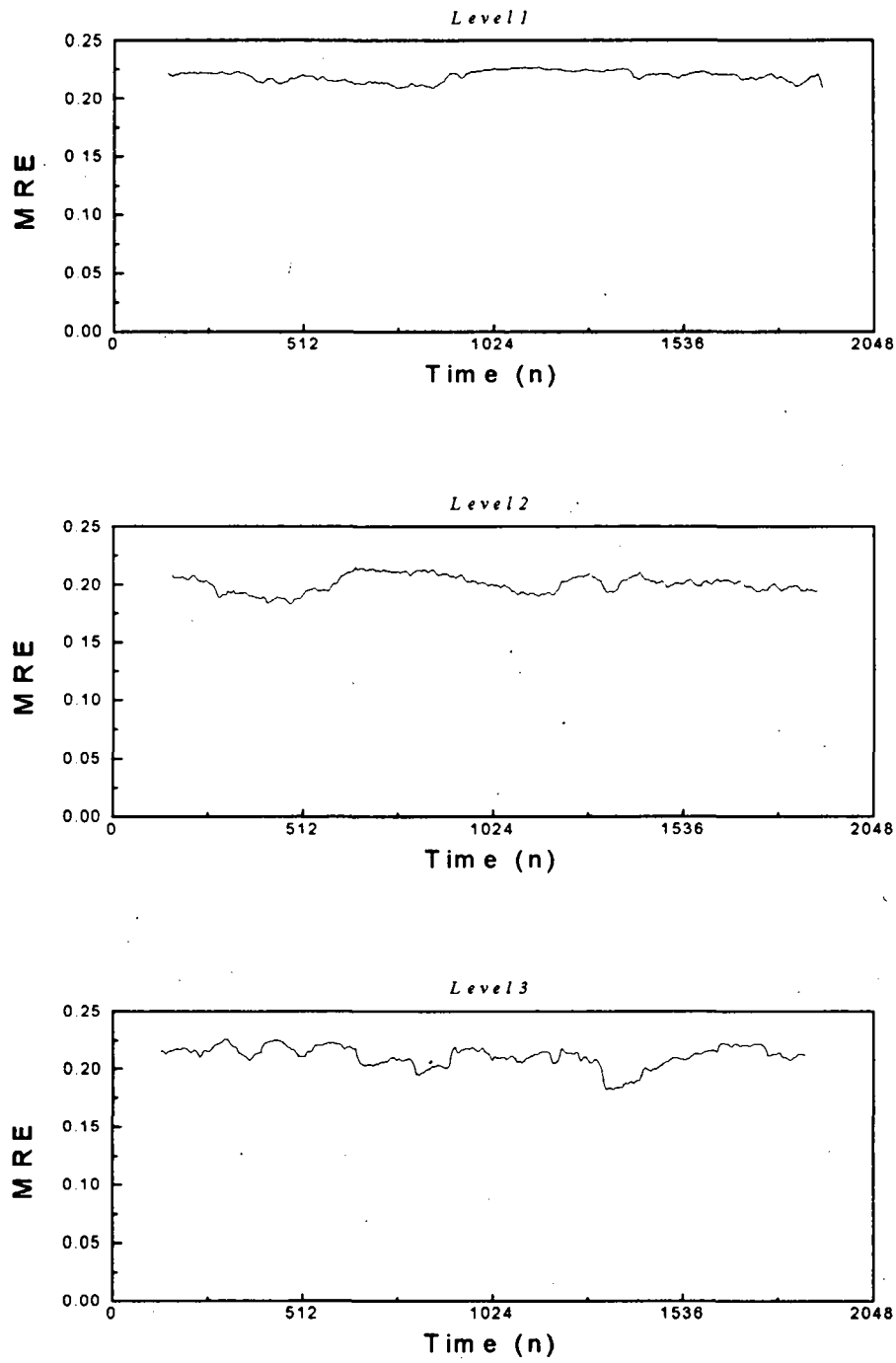

Figure 9: MRE evolution of the cuadratic map signal in Figure 7. The MRE keeps without any perceptible *jump* at its three first levels.

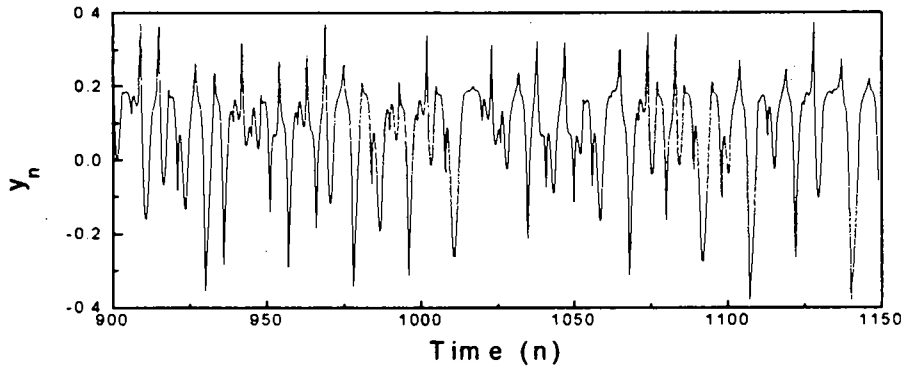

Figure 10: Temporal evolution for the first state of Henon Map equation (eq. 20), with fix parameters $a = 1.4$ and $b = .3$.

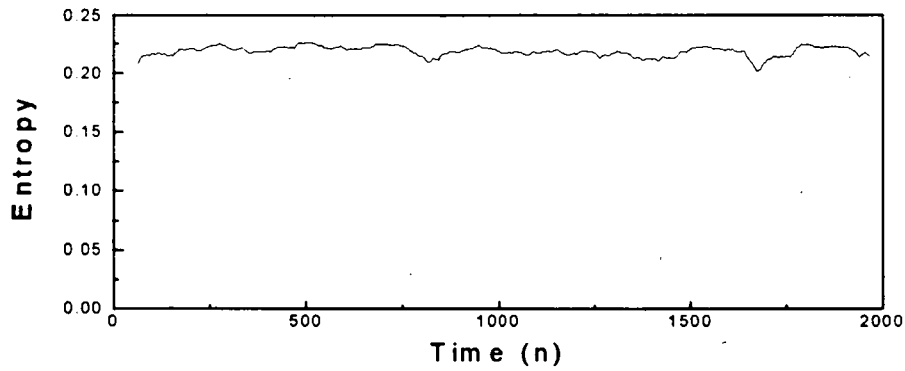

Figure 11: Entropy temporal evolution for the first state of Henon Map equation (eq. 20), with fix parameters $a = 1.4$ and $b = .3$.

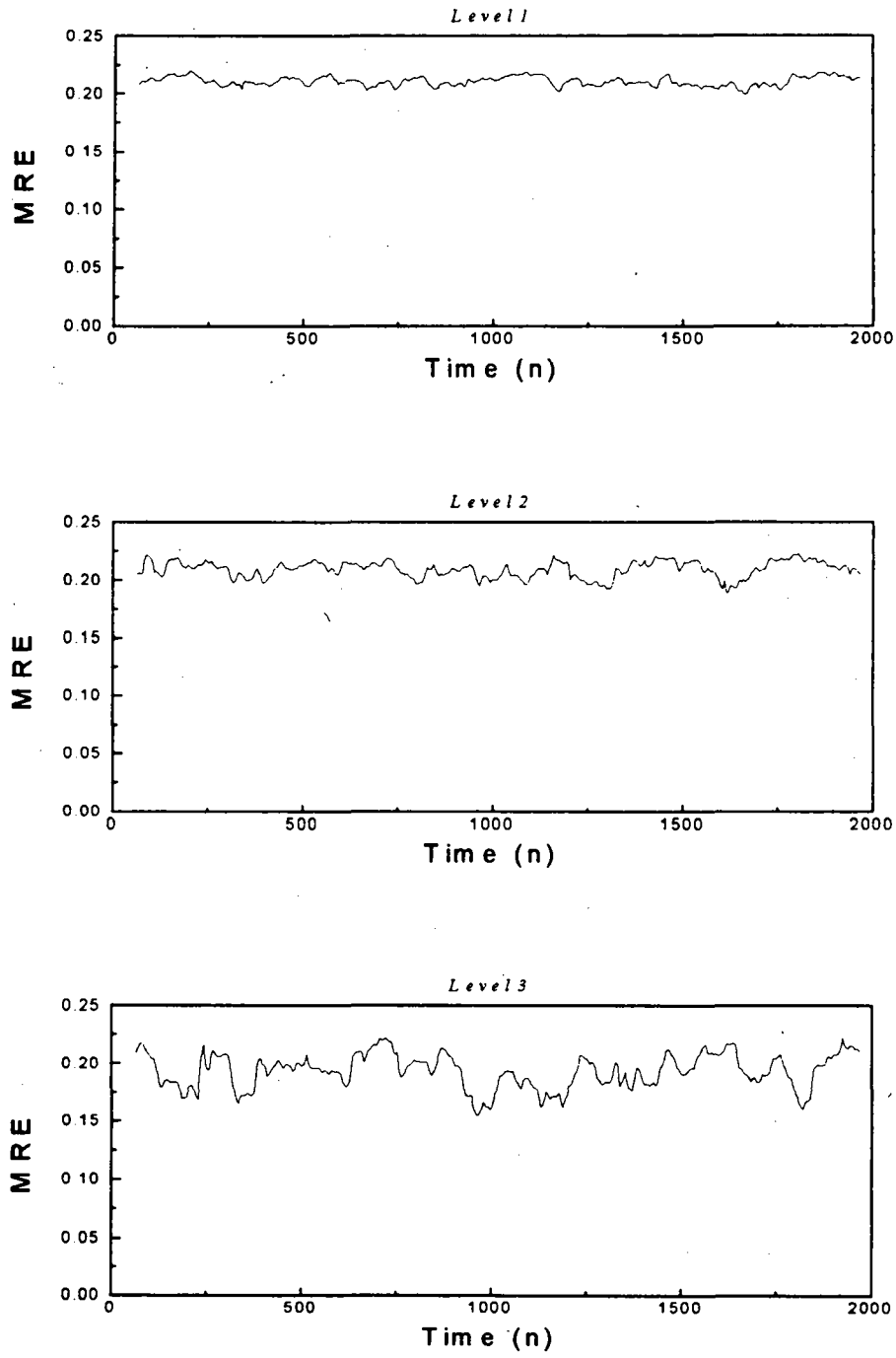

Figure 12: MRE temporal evolution for the first state of Henon Map equation (eq. 20), with fix parameters $a = 1.4$ and $b = .3$.

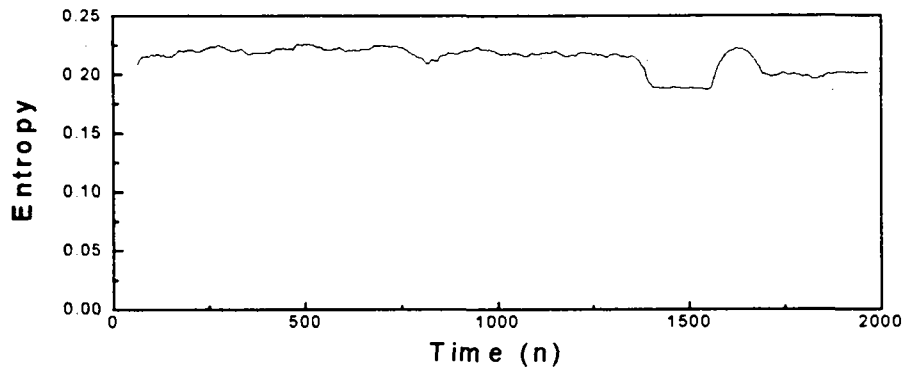

Figure 13: Entropy temporal evolution for the first state of Henon Map equation (eq. 20), with parameters changing as in eq. 17.

value R_1 is $L_1 = 2.16$, $L_2 = 0.0$ and $L_3 = -32.4$ [22], so we have a chaotic dynamic for the initial value R_1 of the parameter.

i) Figure 19 shows the first state of the model (21) solved using four order Runge-Kutta method, with a step $\Delta\, t = 0.01$ and initial values $x(0) = 10$, $y(0) = 1$, $z(0) = 0$, and constant parameter $R_1 = 45.92$. Figures (20) and (21) show the entropy and MRE evolution. We observe that both, the entropy and the MRE follow the geometrical changes of the signal.

ii) In figure 22 we show the first state of the model (21). $R(t)$ is used as a variable parameter, changing according to a continuous version of (17), with $R_1 = 45.92$, $R_2 = 55.92$, $t_1 = 980$ and $t_2 = 1020$. The Lyapunov spectrum for the initial value R_1 is $L_1 = 2.16$, $L_2 = 0.0$ and $L_3 = -32.4$ [22], so we have a chaotic dynamic for the initial value R_1 of the parameter. The entropy (Figure 23) drop around $t = 1000$ is deeper than at the fix parameter case. The MRE presents (Figure 24) the same kind of behavior that we will observe at the eeg signals: a simultaneous drop, in this case at the two first resolution levels.

iii) In figures 26, 27, 28 and 28 it is possible to appreciate that neither the entropy, nor the MRE present any particular feature in front of a linear

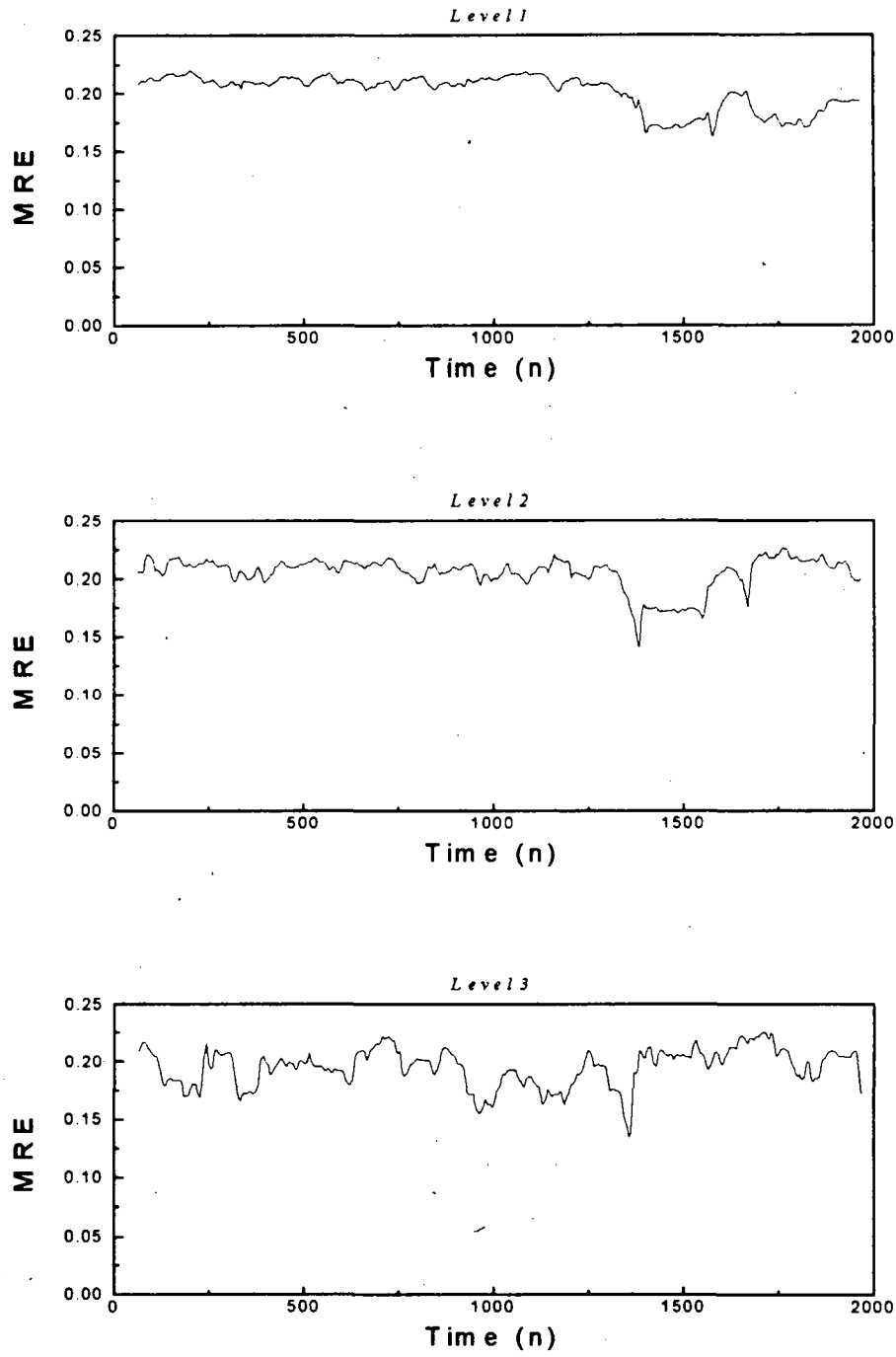

Figure 14: MRE temporal evolution for the first state of Henon Map equation (eq. 20), with parameters changing as in eq. 17.

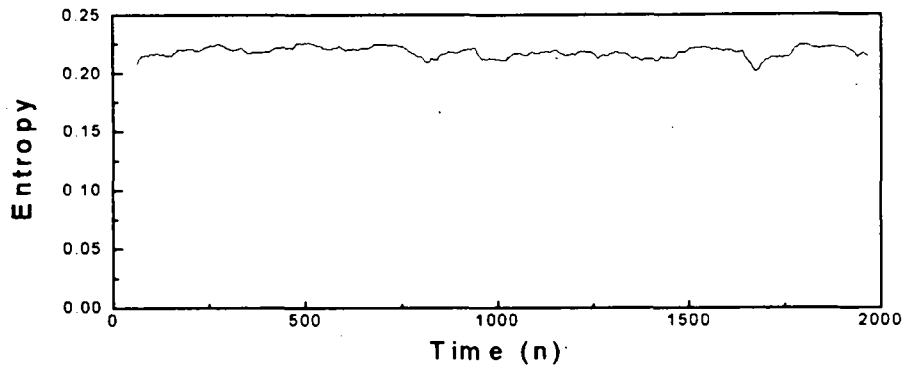

Figure 15: Entropy temporal evolution corresponding to the first state of the system (20), with a linear perturbation of the output signal as in eq. 18.

change of the output signal eqs.(18) and (19), for fix parameters, at the corresponding temporal localization, besides what we have already observed at the signal itself (Figure 19).

4.3 Case II: Electroencephalographic signal

Some physiological systems behaves in a nonlinear chaotic fashion, and different methods have been developed to determine the presence of an attractor, its dimension, and the values of the Lyapunov exponents. In this case we present an example of EEG signals corresponding to epileptic patients. Some authors have shown that the variability of the EEG signals does not represent noise but an attractor ([1], [2], [9]). As it was pointed out by Iasamedis et. al. [7], electrocorticograms of partial epilepsy of temporal lobe origin indicate that the epileptogenic focus also generates signals characteristic of a nonlinear dynamic system. Iasamedis et al. [6] established that during the preictal period, signals from each electrode exhibit positive values of the first Lyapunov exponent L_1, with multiple transient drops; at the onset of the seizure, signals show a simultaneous drop in L_1 to its lowest value.

The stereo electroencephalography (SEEG) (Bancaud and Talairach, 1952) intends to measure the electrical activity of the brain in a three-dimensional way. In each patient the strategy of the implanted electrodes is planned

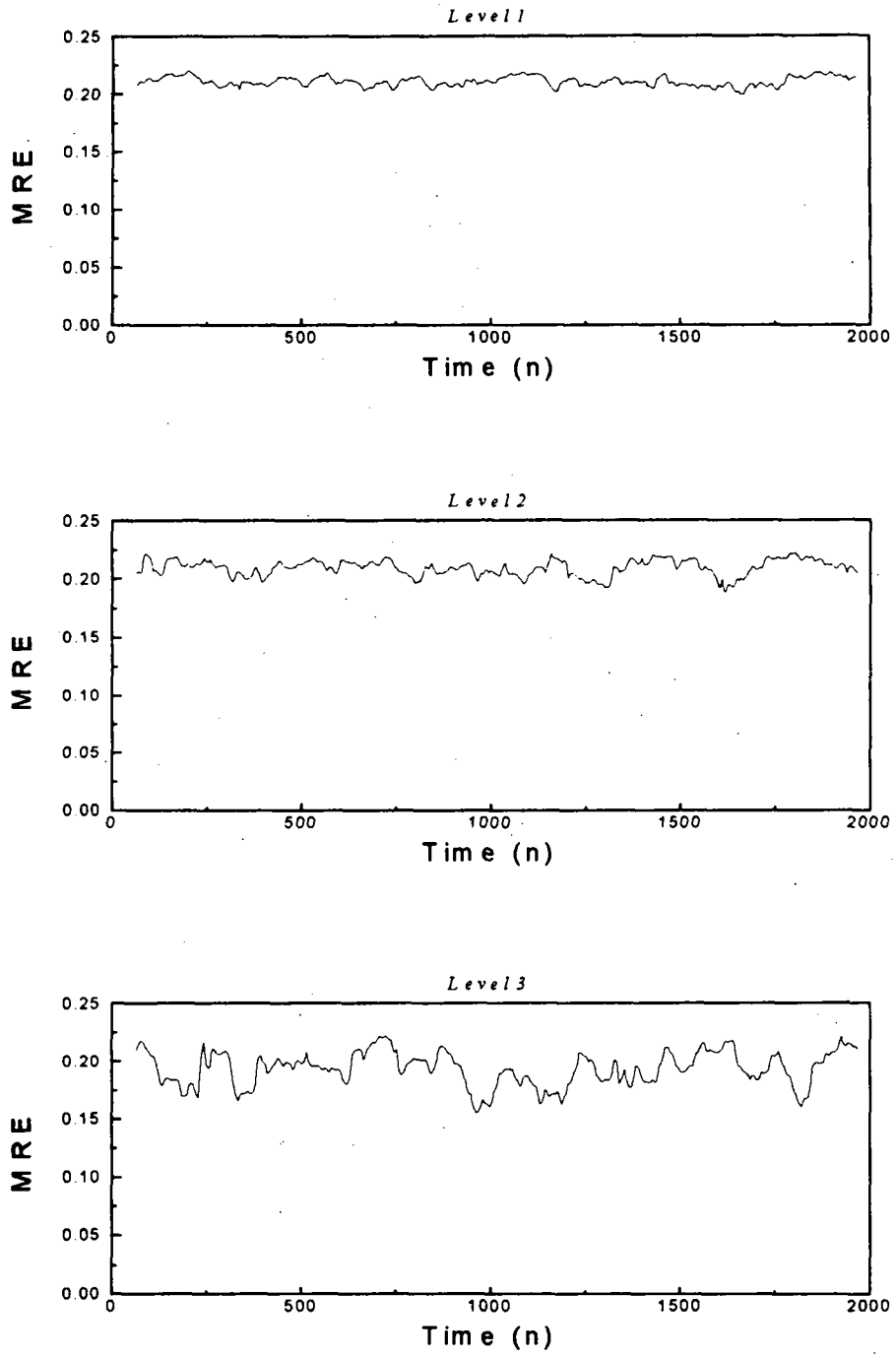

Figure 16: MRE temporal evolution corresponding to the first state of the system (20), with a linear perturbation of the output signal as in eq. 18.

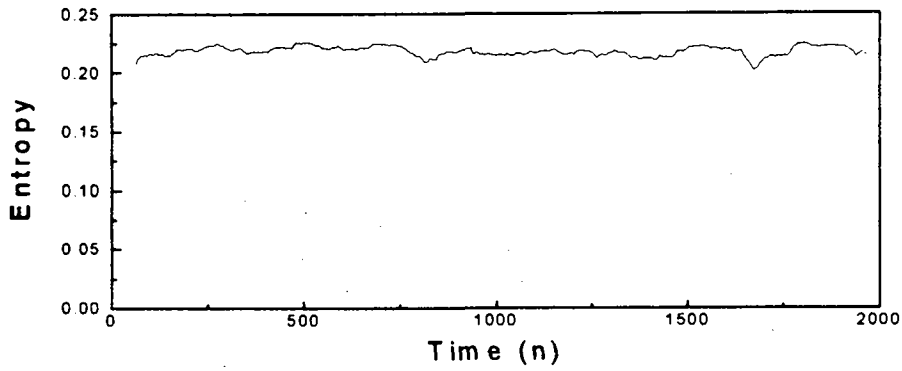

Figure 17: Entropy temporal evolution for the first state of Henon Map (eq. 20), with fix parameters, and the output signal x_n changing as in eq. 19, at $n_0 = 1000$; $c_n = 0.1$.

according to the spatial and temporal organization of the ictal discharges that are simultaneously correlated with clinical symptomatology. The EEG records presented correspond to patients who were explored with 12 multilead electrodes, with length 2 cm. and 1.5 mm. diameter. The analysis of interictal and ictal data is accomplished by visual analysis of the SEEG record. Each signal was amplified and filtered using a 1-40 Hz band-pass filter. A four-pole Butterworth filter was used as low-pass filter, serving as an anti-aliasing scheme. The SEEG was digitalized at 256 Hz through a 10 bits A/D converter.

In preliminar papers ([16],[17]) we have shown that the MRE offers an alternative method for the analysis of EEG signals, corresponding to epileptic patients. Figure 30 shows one channel of an epileptic seizure beginning with a spike followed by a spike-wave paroxysm. The mark was made by the physiologist and corresponds to the starting point of the seizure activity. The frequency distribution of this signal suggests the presence of chaos which is confirmed by the presence of a strange attractor at the phase space diagram (Figure 31) obtained by the time delay method [14]. It is assumed the real time data embedded in a $p = 7$ phase space. Even if the signal entropy time evolution shows several drops (Figure 32), it is difficult to obtain information

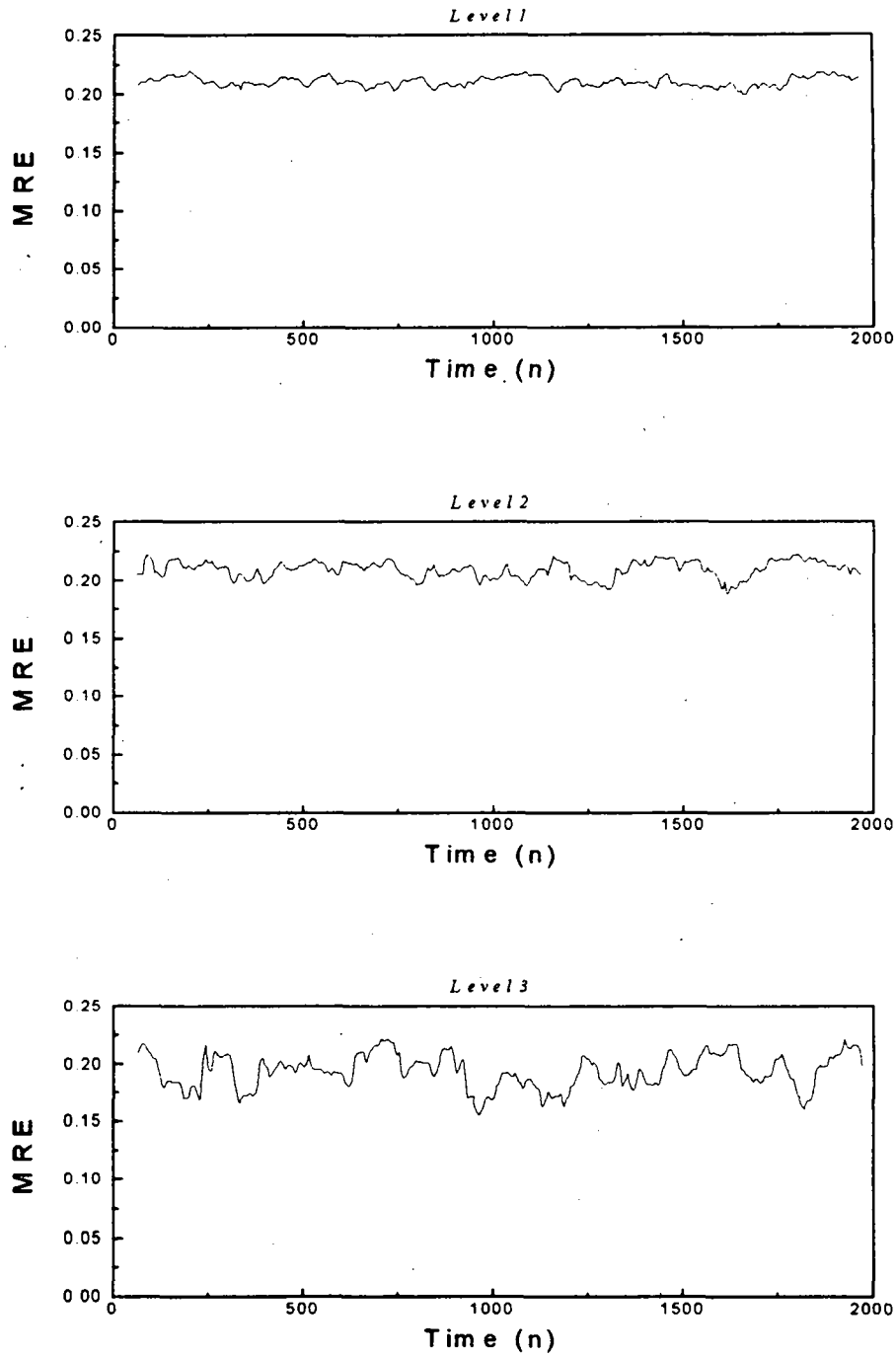

Figure 18: MRE temporal evolution for the first state of Henon Map (eq. 20), with fix parameters, and the output signal x_n changing as in eq. 19, at $n_0 = 1000$; $c_n = 1.1$.

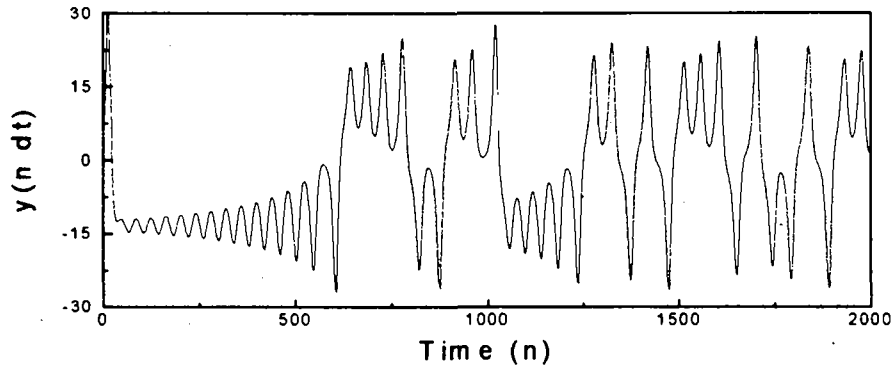

Figure 19: First state temporal evolution of the model (eq. 21) solved using four order Runge-Kutta method, with a step $\Delta\ t = 0.01$ and initial values $x(0) = 10$, $y(0) = 1$, $z(0) = 0$.

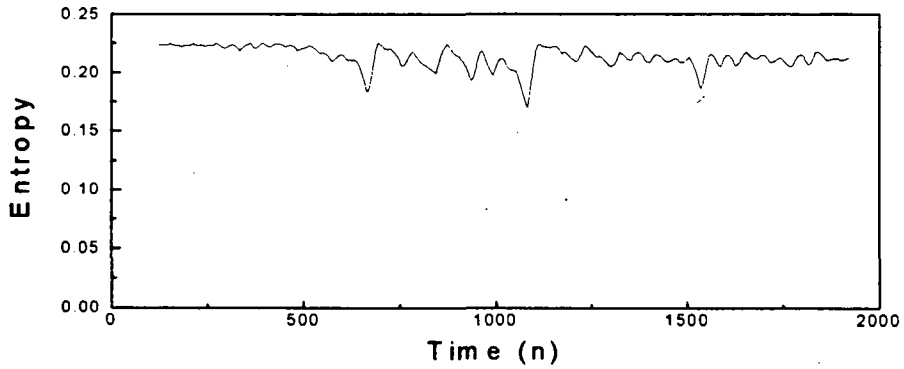

Figure 20: Entropy time evolution of the signal shown in figure 19.

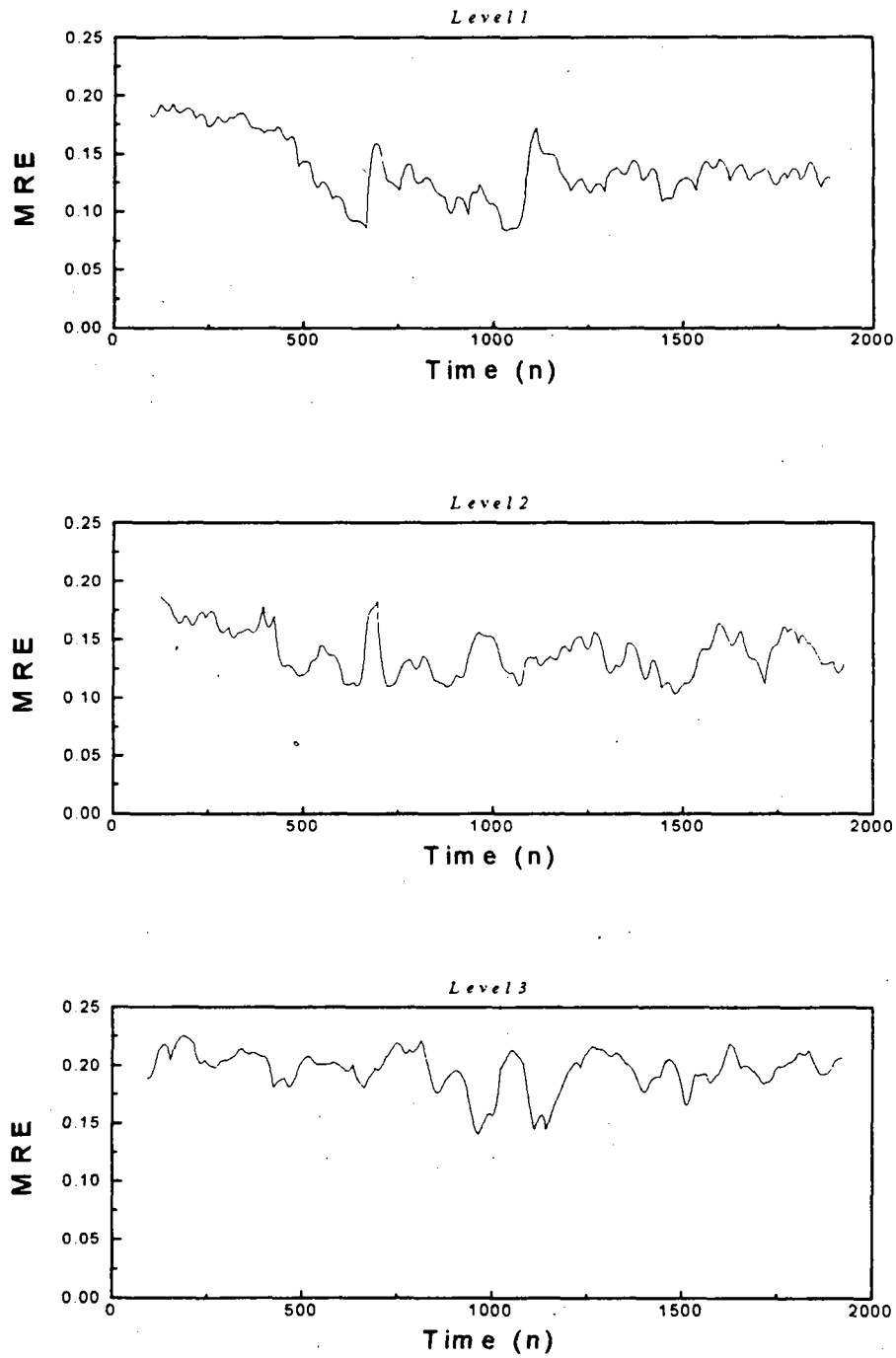

Figure 21: MRE time evolution of the signal shown in figure 19.

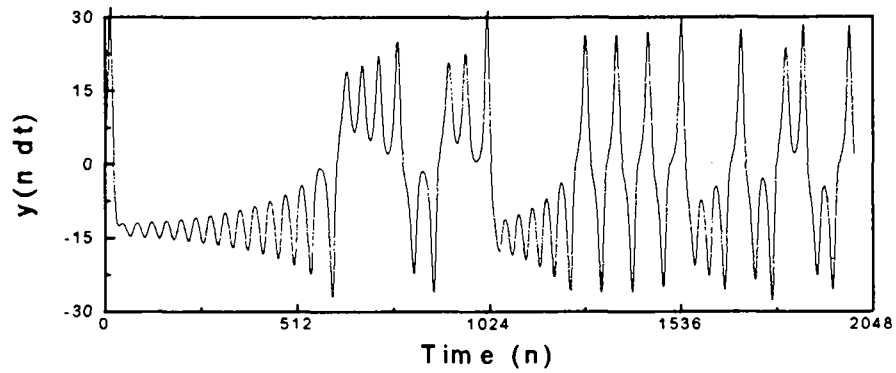

Figure 22: First state temporal evolution of the model (eq. 21) solved using four order Runge-Kutta method, with a step $\Delta\, t = 0.01$, initial values $x(0) = 10$, $y(0) = 1$, $z(0) = 0$ and $R = R(t)$, according to a continuous version of eq. 17.

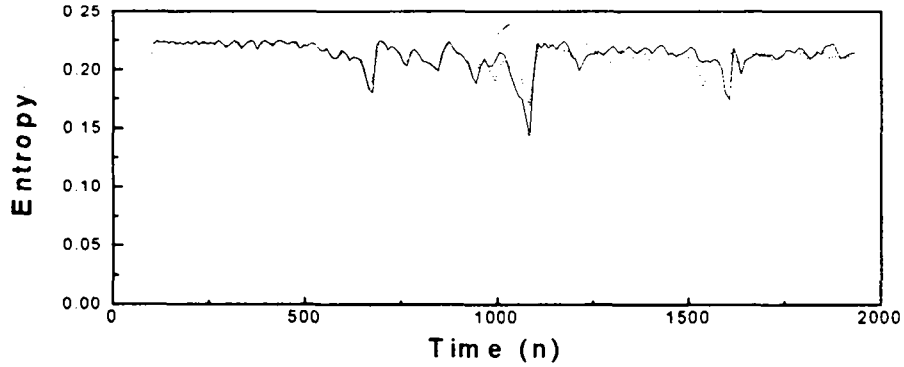

Figure 23: Entropy time evolution for the signal shown in figure 22, compared with Figure 20 (in dot line)

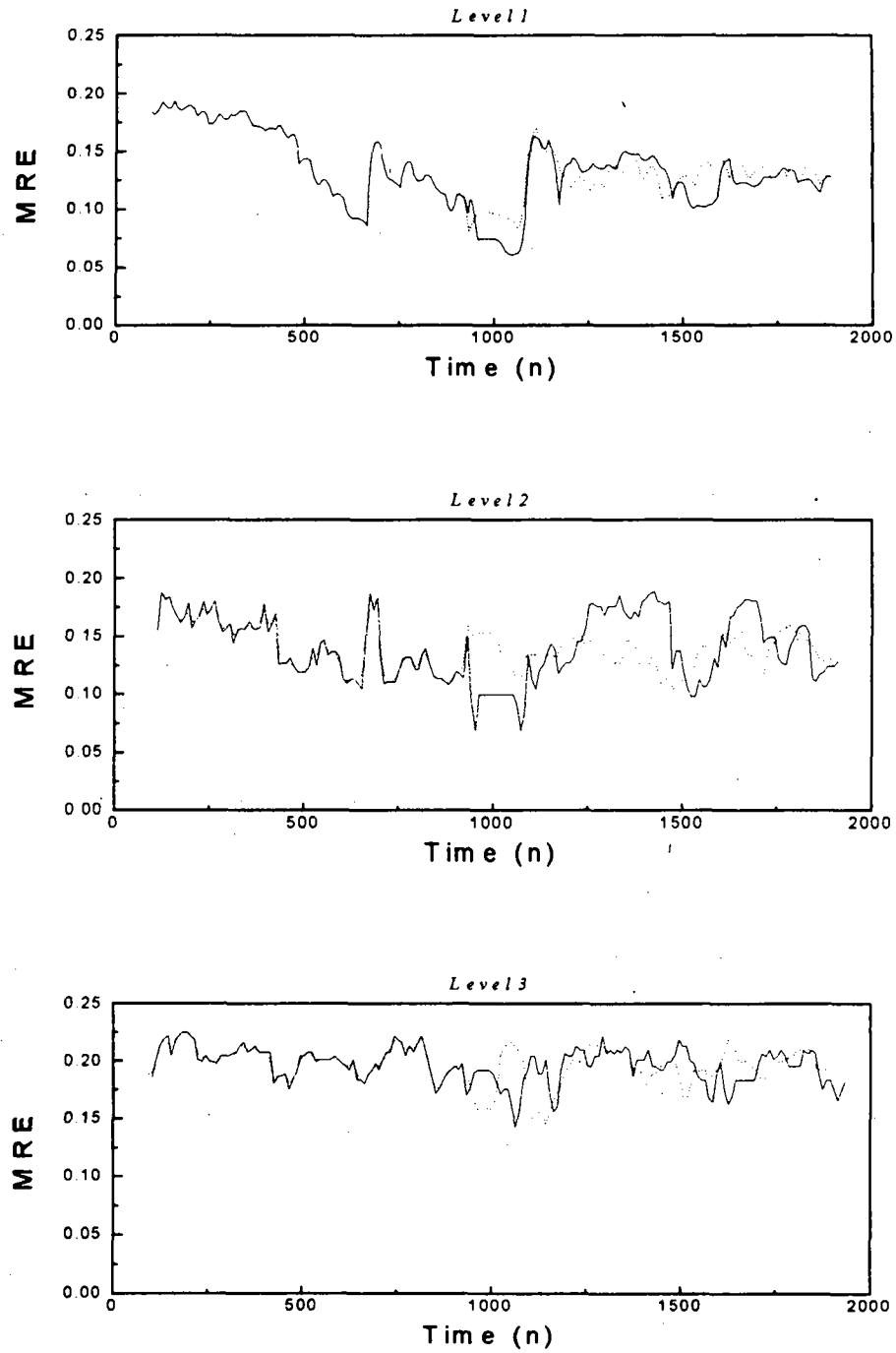

Figure 24: MRE time evolution for the signal shown in figure 22, compared with Figure 21 (in dot line)

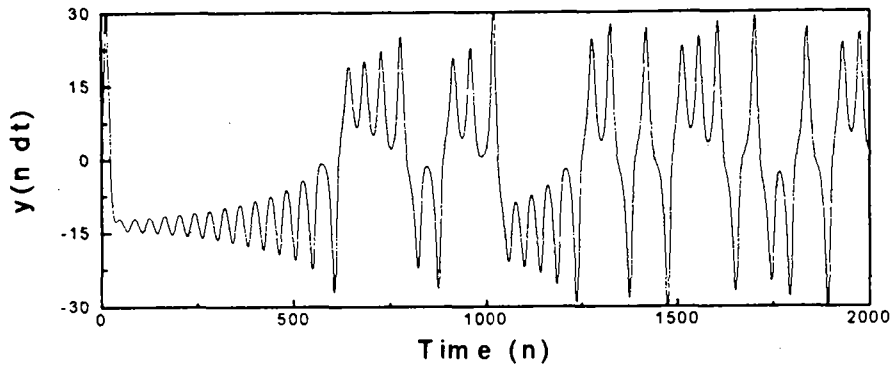

Figure 25: Linear perturbation (eq. 19) at the output signal shown in figure 19.

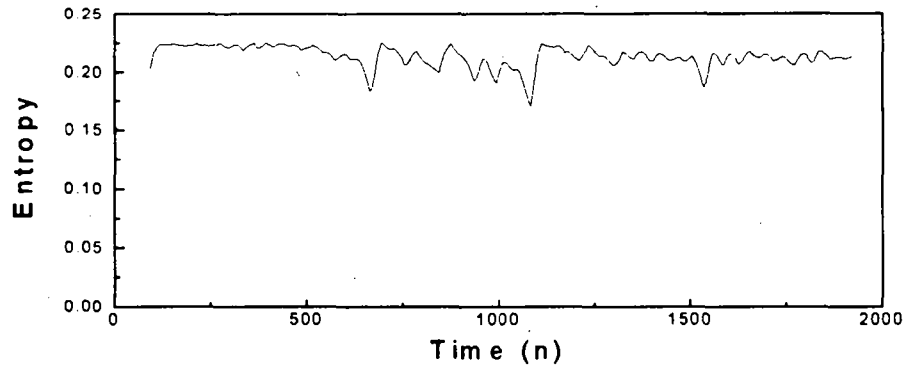

Figure 26: Entropy time evolution for the signal shown in figure 25, compared with Figure /reffig:elorenzy1

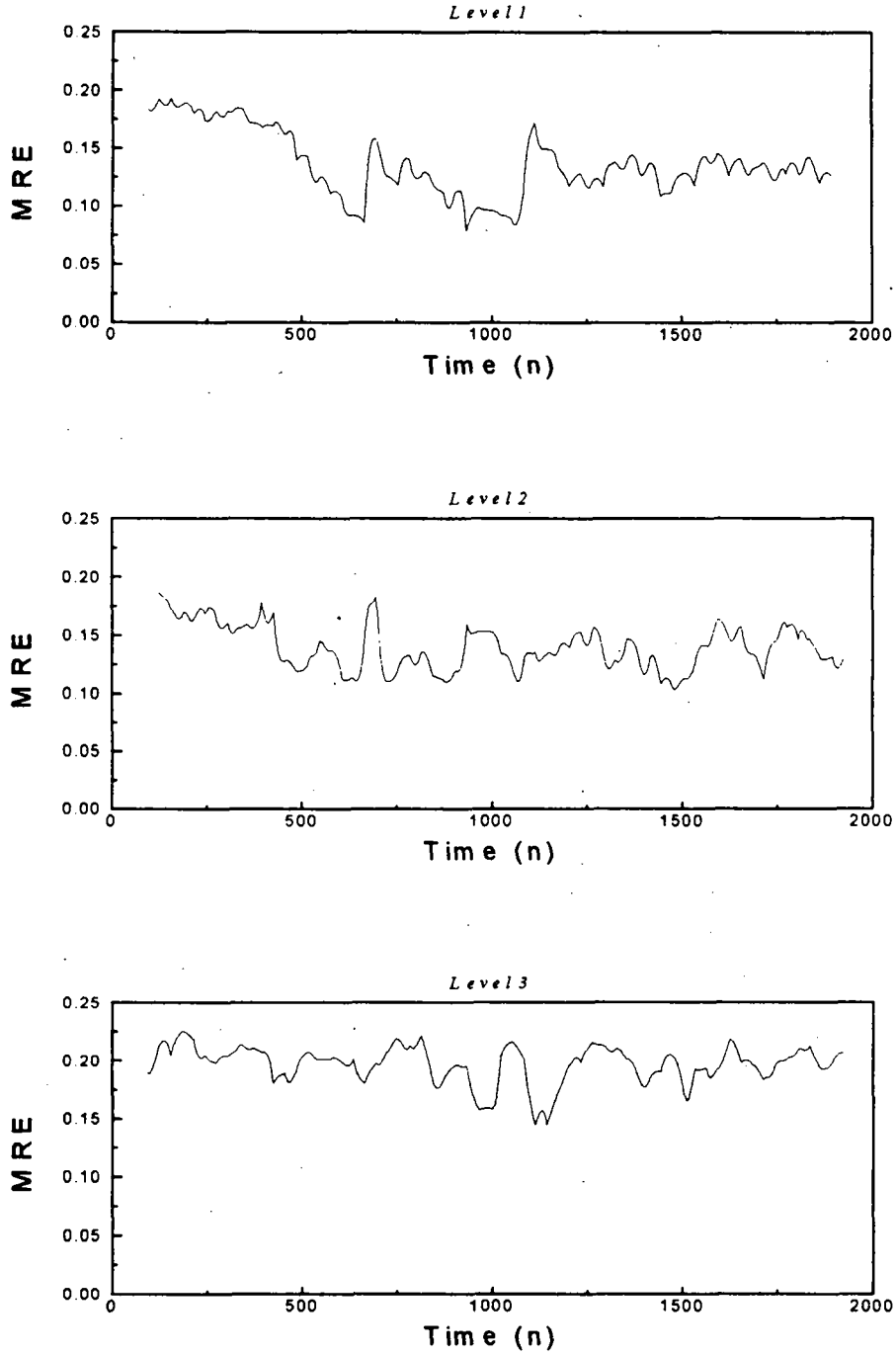

Figure 27: MRE time evolution for the signal shown in figure 25

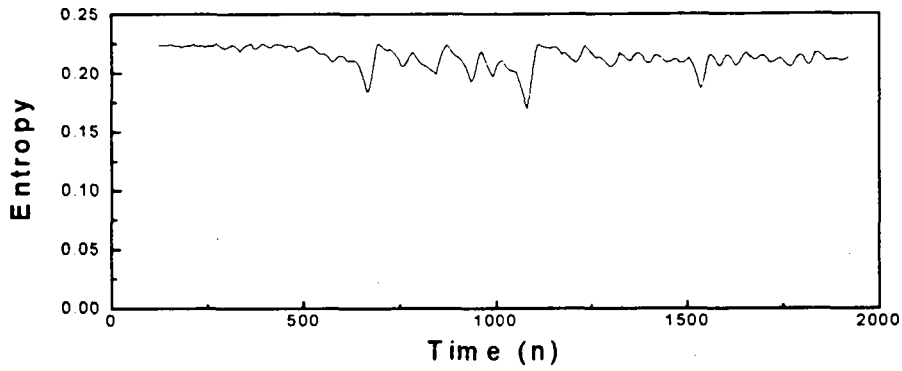

Figure 28: Entropy time evolution for a linear perturbation (eq. 19) at the output signal shown in figure 19

about the seizure onset localization.

Figure 33 shows the MRE time evolution of the signal shown in figure 30 at the three first resolution levels, obtained with $w = 128$ and $\Delta = 5$. At the seizure onset it suffers a sudden drop at the first level to its minimum value. This slope is preceded by similar ones of less magnitude at the three first levels which corresponds to the spike paroxysm shown by the first arrow. The first drop has been observed at other channels of the EEG at which only the spike paroxysm is present. It can be observed that the MRE increases its value again, oscillating between the same values while the EEG signal is arranged at a spike-wave paroxysm as the seizure evolves. Iasamedis [6] established a similar behavior using Lyapunov exponents (Figure 34). Comparing the EEG shown in figure 30 with the MRE time evolution drop (Figure 33), it is clear the agreement between them at the onset of the epileptic seizure.

5 Conclusion

We have developed a method using a multiresolution analysis approach. This method has the localization properties of the wavelets, so it is useful in detecting changes. The results obtained with nonlinear discrete and continuous models at chaotic parameters range suggest that the MRE method must be

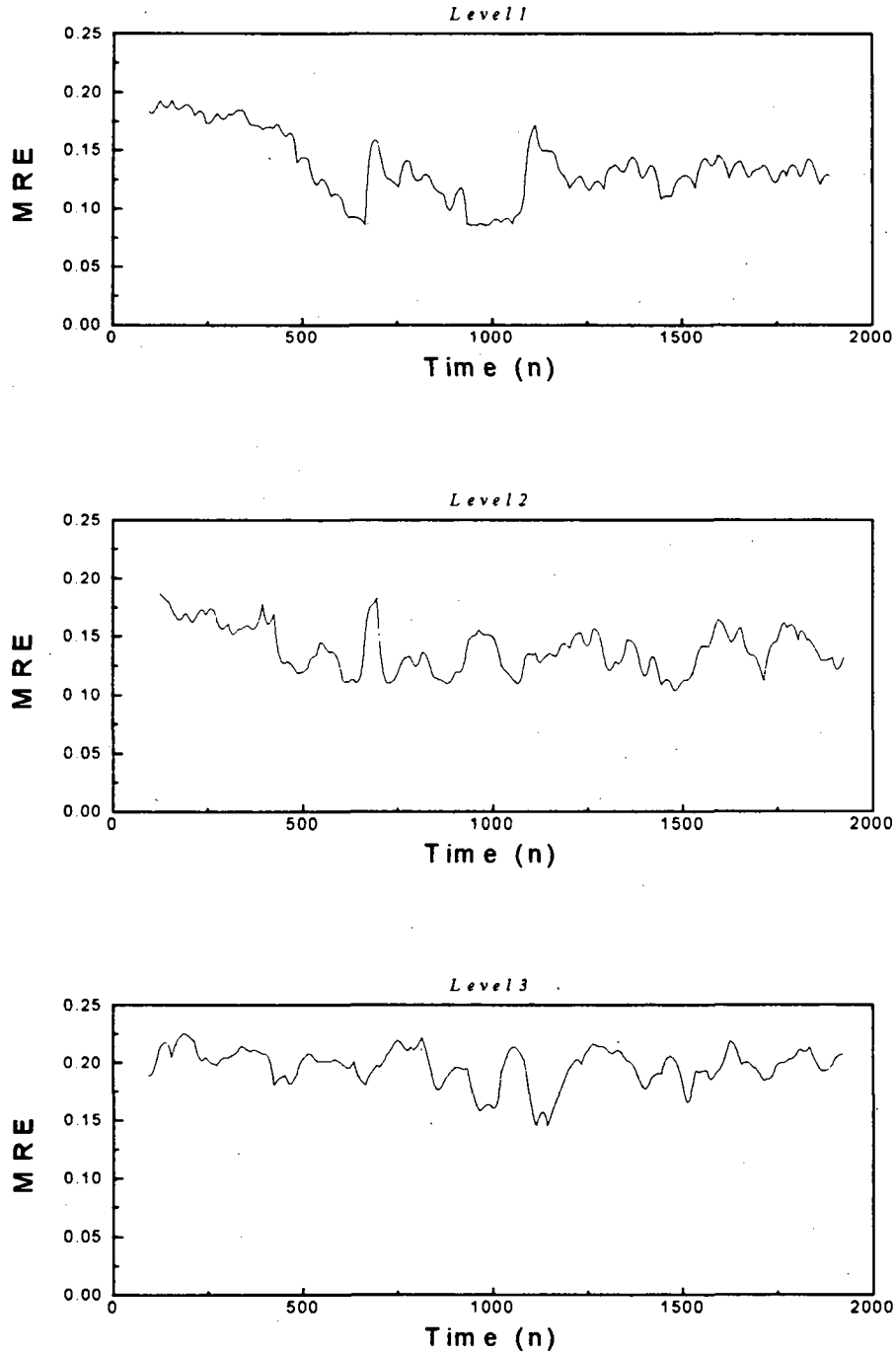

Figure 29: MRE time evolution for a linear perturbation (eqs. 19) at the output signal shown in figure 19

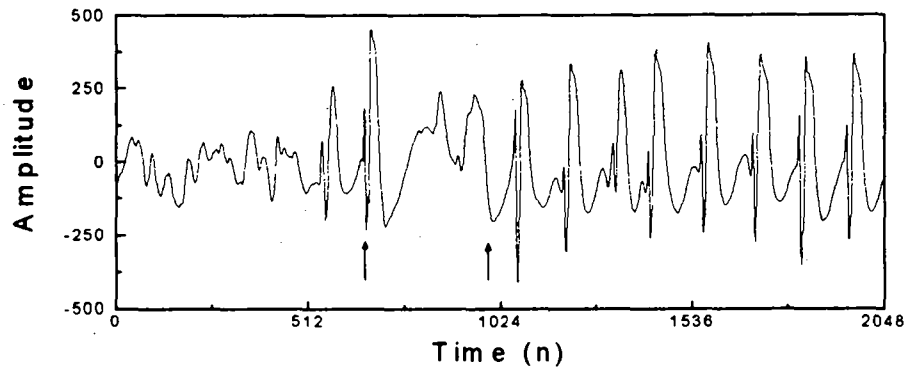

Figure 30: EEG showing an epileptic seizure beginning by a spike paroxysm followed by a spike-wave paroxysm.

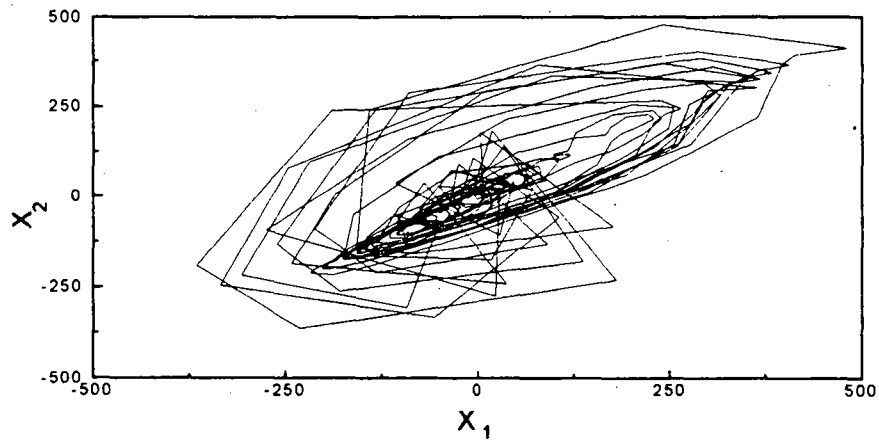

Figure 31: Phase space portrait of the EEG shown at figure 30.

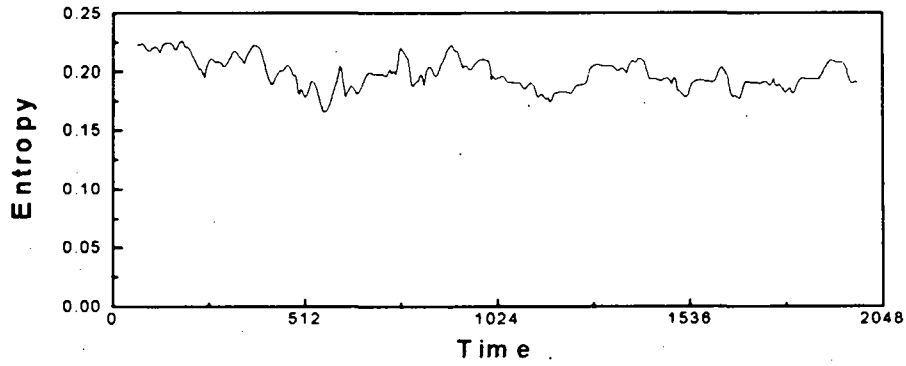

Figure 32: Entropy time evolution of EEG signal (Figure 30).

considered as complement or alternative for detecting changes in the parameters of the system.

Both the entropy and the MRE have shown to be useful for detecting changes in simulated systems. However, the studied cases show that the proposed method allows to distinguish between changes in one parameter and linear perturbations at the output of the system.

In the case of EEG signals, we could establish a suitable agreement between the seizure onset localization obtained by visual inspection, the Lyapunov exponent method and the MRE method proposed in this paper. Further more, the sub-band decomposition of the signal should allow to establish a differentiation between frequency levels, and thus at which ones the transition suggested by Pijn [12] and West ([20],[21]) from one chaotic system to another of different complexity level is dominant.

The main advantage of the entropy and MRE method, compared with Iasamedis' method for evaluating the Lyapunov exponents, in the goal of detecting changes in the signal, is that it allows the analysis with short signal segments with less computational cost. The last one is very high due to the algorithm complexity and the fact of requiring a register segment of around 10^D to 30^D points, where D is the attractor dimension. For example, in the EEG case presented here, D is between 2 and 3 at the ictal case [7]. So the record length must be around 20 min., starting 10 min. before the

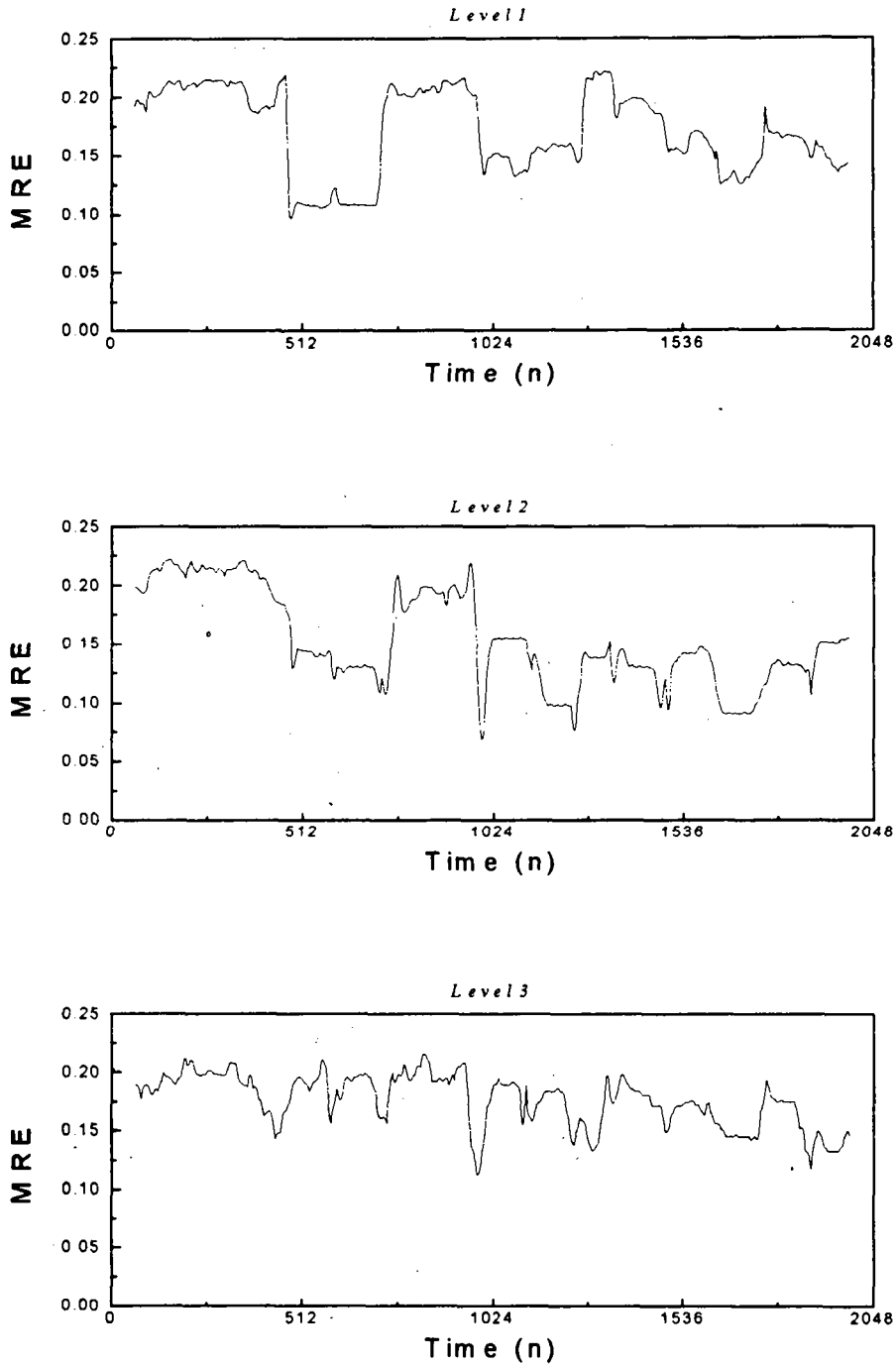

Figure 33: MRE time evolution of EEG signal (Figure 30).

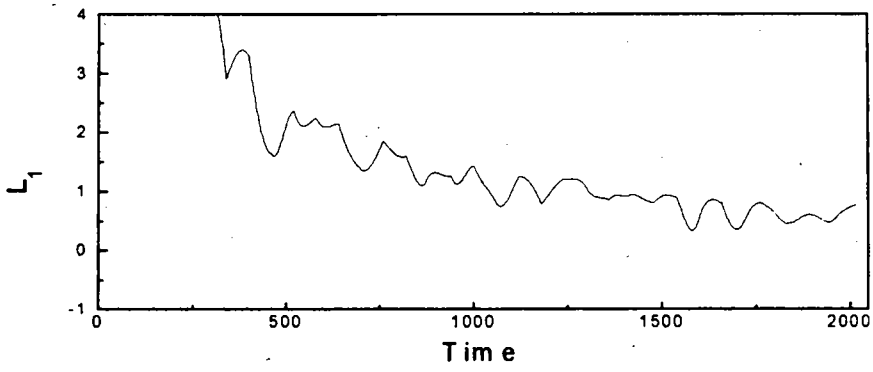

Figure 34: First Lyapunov exponent of EEG signal (Figure 30), computed using Wolf's algorithm with Iasamedis' modification.

seizure onset. With the method here proposed, 8 s analysis windows were used. The algorithms have been implemented in Mathematica 2.2 and run on a PC-486 DX2 (66 MHz). For an EEG segment of 3180 samples, the CPU time for the evaluation of the temporal evolution of L has been of 61706 s. The corresponding CPU time for the MRE has been of 246 s. The former has been evaluated with Iasamedis algorithm ([6]) with a temporal evolution of 20 samples. For most of the MRE evaluations here presented the parameters have been $\Delta = 5$, $w = 128$ and $M = 10$. A modification in the values of w and Δ produce a zoom-in or zoom-out efect in the results observed at the MRE evolution.

6 Acknowledgements

The authors would like to thank the Authorities of INRIA for the support given in the opportunity of the sojourn of María Eugenia Torres at INRIA-Rocquencourt. To the Coordinators of the Cooperation-Project that connects INRIA with Argentine Universities and Scientific Institutes, E. Rofman and R. Gonzalez. And to the Authorities of the Universidad Nacional de Entre Ríos for their support.

References

[1] Babloyantz A., *Evidence of chaotic dynamics of brain activity during the sleep cycle*, In Meyer-Kress G. (Eds.): Dimensions and Entropies in Chaotic Systems. Berlin, Springer Verlag, 241-245. 1986.

[2] Basar E., Chaos in Brain Function. Berlin, Springer Verlag, 1990.

[3] G. Benettin, L. Galgani and J.M. Strelcyn, *Lyapunov characteristic exponents for smooth dynamical systems and for Hamiltonian systems: a method for computing all of them*, Meccanica, 15 , 9. 1980.

[4] Chui Ch., "An Introduction to Wavelets ", in Wavelet Analysis and its applications, Ch. Chui, Series Editor. Academic Press, 1992.

[5] D 'Attellis C. E., Isaacson S. I., Sirme R. O., *"Algorithm for detecting epileptic events in EEG's using wavelet theory"*, Proceedings "VI Reunión de Trabajo de la Información y Control ", Vol.1, pp 24-29, Nov. 1995,

[6] L.D.Iasamedis, C. Sackellares, H. Zaveri and W. William's, *"Phase space topography and the Lyapunov exponent of electrocorticograms in partial seizures"*, Brain Topography, Vol. 2, No 3, 1990.

[7] L.D.Iasamedis, C. Sackellares, H. Zaveri and W. William's, *"Modellingof ECoG in temporal lobe epilepsy"*, 25th Ann. Rocky Mountain Bioing. Symposium, 1201-1203,1988.

[8] Meyer, Y.: "Wavelets. Algorithms and applications".SIAM, 1993.

[9] Meyer-Kress G., Layne S. C., Dimensionality of human electroencephalogram, S. H. Koslow, A. J. Mandel, M. F. Shlesinger (Eds): Perspectives in Biologycal Dynamics and Theoretical Medicine. Ann. N.Y. Acad. Sci., 504, 1987.

[10] Oseledec, V.I., *" A multiplicative ergodic theorem. Lyapunov characteristic numbers for dynamical systems"*, Trudy Mosk.Mat.Obsc.19,179 (Moscov Math. Soc., 19,197),1968.

[11] Pesin Y. B., Russ. Math. Surv., 32, 4, 55 ,1977.

[12] Pijn J. P. M., Lopez da Silva F. H., *"Propagation of electrical activity: nonlinear associations and time delays between EEG signals"*, S. Zschocke, E. J. Speckmann (Eds), Basic Mechanism of the EEG. Boston, Bishauser, 1993.

[13] I. Shimada and T. Nagashima, *A numerical approach to ergodic problem of dissipative dynamical system*, Prog. Thor. Phys. 61,1605, 1979.

[14] Takens F., *"Detecting strange attractors in turbulence"*, Randand D.A., Young L.S. (Eds.), Dynamical systems and turbulence, Lecture Notes in Mathematics. Berlin, Springer Verlag, 366-381,1981.

[15] Thompson J.M., Stewart, "Non linear Dynamics and Chaos ". Ed. Wiley and Sons. 1993.

[16] Torres M., Gamero L. , DAttellis E., *"A multirresolution entropy approach to detect epileptic form activity in the EEG"*. Proceedings 1995 IEEE Workshop on non linear signal and image processing, Vol II, pp791-794, Ed. I. Pitas,1995.

[17] Torres M., Gamero L. , DAttellis E, *"Pattern Detection in EEG using multirresolution entropy"*, Latin American Applied Research, 25: 53-57, 1995.

[18] Unser M., Aldroubi A., Murray E., *"A family of polynomial spline Ondita Transform "*, Signal Processing 30, 141-162, Elsevier, 1993.

[19] J. Van Neerven, "Determination of the correlation dimension from a time series, applications to rat EEGs: sleep, theta rythm and epilepsy". Master's thesis. Dept. Exp. Zoology, Univ. of Amsterdam, Amsterdam, 1988.

[20] West B. J., Fractal Physiology and Chaos in Medicine, Nonlinear Phenomena in Life Science, B. J. West (Eds), World Scientific, 1, Singapore, 1990.

[21] West B. J., Patterns, Information and Chaos in Neuronal Systems, Nonlinear Phenomena in Life Science. World Scientific, 2, Singapore, 1993.

[22] Wolf A., Swift J. B., Swinney H. L., Vastano J. A., *"Determining Lyapunov exponents from a time series"*. Physica D, 16, 285-317, 1985.

Unité de recherche INRIA Rocquencourt
Domaine de Voluceau - Rocquencourt - B.P. 105 - 78153 Le Chesnay Cedex (France)

Unité de recherche INRIA Lorraine - Technopôle de Nancy-Brabois - Campus scientifique
615, rue du Jardin Botanique - B.P. 101 - 54602 Villers lès Nancy Cedex (France)
Unité de recherche INRIA Rennes - IRISA, Campus universitaire de Beaulieu 35042 Rennes Cedex (France)
Unité de recherche INRIA Rhône-Alpes, 46, avenue Félix Viallet - 38031 Grenoble Cedex 1 (France)
Unité de recherche INRIA Sophia Antipolis - 2004, route des Lucioles - B.P. 93 - 06902 Sophia Antipolis Cedex (France)

Éditeur
INRIA - Domaine de Voluceau - Rocquencourt - B.P. 105 - 78153 Le Chesnay Cedex (France)

ISSN 0249 - 6399